International Journal of Multiphase Flow 35 (2009) 277–287

Contents lists available at ScienceDirect

International Journal of Multiphase Flow

journal homepage: www.elsevier.com/locate/ijmulflow

Light multiple scattering correction of laser-diffraction spray drop-size distribution measurements

C. Dumouchel *, P. Yongyingsakthavorn, J. Cousin

CNRS UMR 6614 – CORIA, Université et INSA de Rouen, Avenue de l'Université, B.P. 12, 76801 Saint Etienne du Rouvray, France

ARTICLE INFO

Article history:
Received 4 August 2008
Received in revised form 31 October 2008
Accepted 1 November 2008
Available online 12 November 2008

ABSTRACT

This paper reports an experimental investigation on the practical use of a laser-diffraction instrument, the Malvern Spraytec 2007 to characterize sprays produced by a high-pressure GDI injector. The sprays are highly transient, large, composed of very small drops, dense and heterogeneously distributed in space. These characteristics are at the origin of undesirable effects (beam steering, vignetting and light multiple scattering) whose manifestations are experimentally identified. Ignoring the diodes concerned by beam steering erases the effect of this phenomenon but vignetting and light multiple scattering effects combine to bias the measurements and both require to be corrected. A *n*th order empirical correction procedure, based on the analysis of the light intensity distribution, is developed. It is a generalization of a second order procedure presented in a previous investigation. The increase of the correction order is demonstrated to be necessary when the injection pressure is greater than 11 MPa. The application of this correction procedure reported that light multiple scattering affects laser-diffraction when the transmission is less than 40%. This limit is in agreement with investigations of the literature and gives credit to the empirical correction procedure. Despite the correction procedure is applicable for the present operating conditions only, this work defines an experimental protocol to apprehend laser-diffraction spray characterization in severe operating conditions and that can be reproduced with ease. Furthermore, it is emphasized that the combination of the Spraytec and the correction procedure performances allows cycle-to-cycle spray drop-size distribution variations to be determined. Such information is of paramount importance and the Spraytec is probably the sole instrument able to provide it.

© 2008 Elsevier Ltd. All rights reserved.

1. Introduction

Over the past decades, an extensive literature has been dedicated to the laser-diffraction technique commonly used to investigate liquid sprays. This technique provides a line of sight average measurement of the drop-size distribution. The measurement volume is defined as the intersection of a particle field and a collimated laser beam. A part of the laser beam that passes through the spray is diffracted. In the forward direction, the light falls on a Fourier transform lens: the undiffracted light is focused onto a point on the axis in the focal plane and the diffracted light forms a far-field Fraunhofer pattern around this central spot. The ratio of the undiffracted light intensity I to the incident light intensity I_0 provides the transmission T of the measurement, i.e.,:

$$T = \frac{I}{I_0} \tag{1}$$

As commonly done in the literature, values of the transmission given here after are expressed in percentage. However, when involved in equations, the transmission values range from 0 to 1 as indicated by Eq. (1). The former laser-diffraction instruments (as the particle sizer 2600D from Malvern, UK) were equipped with a series of semi-concentric ring detector to record the diffraction pattern, each ring being associated with a drop diameter interval that was a function of the focal length of the collecting lens, of the dimensions of the rings and of the laser beam properties. Because of the shape of the detectors, the diffraction pattern was axisymmetric and was considered as being the signature of a set of spherical droplets. Thanks to the development due to Swithenbank et al. (1977), a mathematical inversion procedure based on the Fraunhofer diffraction theory calculated the volume-based drop-size distribution that had the same diffraction pattern as the one recorded. Considering the way drops are sampled, this distribution is a spatial frequency of the drops according to their diameter.

Over the past years laser-diffraction instruments have been modified and improved. For instance, the latest version commercialized by Malvern (Spraytec 2007) has detectors that are not semi-concentric anymore: they have much smaller dimension and cover an angular sector only with a surface area that follows a logarithm progression from the center to the outside. Despite this modification, the mathematical inversion procedure still assumes

* Corresponding author. Tel.: +33 2 32 95 36 23.
E-mail address: Christophe.Dumouchel@coria.fr (C. Dumouchel).

0301-9322/$ - see front matter © 2008 Elsevier Ltd. All rights reserved.
doi:10.1016/j.ijmultiphaseflow.2008.11.001

an asymmetric diffraction pattern. Furthermore, the Spraytec 2007 is able to work at an acquisition rate as high as 10 kHz allowing highly transient injection, such as gasoline injection for instance, to be investigated.

As far as the mathematical inversion procedure is concerned, two main differences between former and latter instruments must be emphasized. First, it is now based on the Lorenz–Mie theory that accounts for the contribution to the angular light energy distribution of refraction through small particles. The mathematical inversion procedure based on the Fraunhofer diffraction theory interpreted this portion of light energy as diffracted light and overestimated the small particle population. The use of the Lorenz–Mie theory considerably improves the instrument performances when measuring very fine sprays (Corcoran et al., 2000). Second, the mathematical inversion now includes a patented multiple scattering algorithm. According to Hirleman (1988, 1990), light multiple scattering can occur in two situations: 1 – when the interparticle spacing is so small that the scattering characteristics of a particle depend on the positions and sizes of adjacent particles, 2 – when the optical path (extent in the direction of the incident radiation) is so large that a significant number of photons are scattered more than once before exiting the medium and reaching the detector. As a consequence, the diffraction angles are increased and the initial mathematical inversion procedure, based on the assumption of individual photons scattering off single particles, overestimated the small-drop population and underestimated the width of the distribution.

To remedy this problem, Felton et al. (1985) and Hirleman (1988, 1990) developed light multiple scattering models. Felton et al.'s (1985) model divides the light path into a sequence of slices of equal transmission and assumes that half of the scattered light goes forward. Furthermore, the spray is assumed to have the same concentration and drop-size distribution in all slices and the photons that are scattered at angles larger than the outermost detector cannot be rescattered back into the detector range. This model was validated on mono-modal and bi-modal size distribution of controlled glass beads suspensions (Felton et al., 1985; Hamidi and Swithenbank, 1986) and it served as a basis to develop multiple scattering correction procedures (Hamidi and Swithenbank, 1986; Gomi, 1986). Cao et al. (1991) extended Felton et al.'s (1985) model paying attention to the scattering of an off-axis beam by the particles. These investigations reported that light multiple scattering affects the measurement when the transmission is less than about 40% and introduces a bias that depends on the transmission and on spray characteristics.

The model developed by Hirleman (1988, 1990) combines the method of successive orders with the discrete ordinates approach similar to the one of Felton et al. (1985). This formulation assumes isolated particle light scattering, an axisymmetric diffraction pattern, spray characteristics (concentration and drop-size distribution) uniformly distributed in space, particles larger than the light wavelength and considers the scattered light in the near-forward direction only. Furthermore, the model was developed for a laser-diffraction instrument with a specific circular diode series arrangement. This model favorably agreed with the conclusions reported by Felton et al. (1985), Hamidi and Swithenbank (1986) and Gomi (1986) concerning the limit in transmission and the influence of the drop-size distribution on the light multiple scattering effects. The correction algorithm implemented in the Malvern instruments has been derived from Hirleman's model (Harvill et al., 1995; Harvill and Holve, 1998) and allows measurements with transmission as low as 5% to be performed.

Several experimental works investigated light multiple scattering effects for variable situations including large sprays (Dodge, 1984; Triballier et al., 2003), controlled glass beads suspensions (Gülder, 1987, 1990; Paloposki and Kankkunen, 1991) and hollow sprays (Boyaval and Dumouchel, 2000, 2001). Light multiple scattering was identified from the effect of a continuously decreasing transmission on spray characteristics such as mean diameters, representative diameters, span factor or light intensity distributions. These experiments confirmed that the limit in transmission above which light multiple scattering is negligible is of the order of 40%. Just below this limit, light multiple scattering effects concentrate on the small-drop population and these effects diffuse to the big-drop population as the transmission decreases. For instance, Paloposki and Kankkunen (1991) found that light multiple scattering effects affect the characteristics diameter $D_{v0.5}$ when T reaches 40% whereas alterations on the $D_{v0.9}$ diameter were observed at $T = 10\%$. These experimental investigations used former Malvern equipments that were not equipped with an optional multiple scattering correction algorithm except the work due to Triballier et al. (2003). Investigating the effect of light multiple scattering on large and inhomogeneous sprays, they reported a poor efficiency of this correction algorithm and recommended to test it before any application.

This work presents an experimental protocol that is recommended to follow when laser light diffraction measurements are performed in severe operating conditions, i.e., large, dense, highly transient and inhomogeneous sprays. The sprays investigated here are those produced by a gasoline direct-injection (GDI) device. First, the undesirable effects of light multiple scattering, vignetting and beam steering are identified. Second, an empirical correction model is developed to correct the measurements from vignetting and light multiple scattering effects. The application of this model allows the Malvern correction algorithm to be tested and the performances of the GDI injector to de determined.

2. Experimental setup and diagnostic

2.1. Experimental setup

Fig. 1 shows the experimental setup. The liquid is kept in a tank where its temperature is maintained at 18 ± 2 °C thanks to a heat exchanger. At the exit of the tank, the fluid is filtered. A combination of two pumps (low pressure (LP) and high pressure (HP) pumps) provides an injection pressure ΔP_i ranging from 0.5 to 20 MPa. The injection pressure is regulated and measured by a high-pressure sensor placed just before the injector. An Engine Control Unit (ECU) operates the injector. Finally, an extraction system collects the droplets out of the testing area. Throughout the study, the liquid used during the experiments is Exxsol D40 (density $\rho_L = 776$ kg/m^3, surface tension $\sigma = 24.7$ mN/m, kinematic viscosity $\nu = 1.3$ mm^2/s, vapor pressure $P_v = 0.24$ kPa).

Zhao et al. (2002) defined two main GDI injector categories, i.e., swirl and non-swirl configurations. The injector investigated in the present study belongs to the second category. It produces a hollow conical issuing flow without imposing an intensive swirling motion on the internal flow. The conical shape is obtained thanks to an appropriate design of the injector nozzle. Contrary to many former GDI injectors, an outward opening needle controls the opening and the closing of the injector. In order to ensure transient phases as short as possible, a piezoelectric actuator commands the injector's needle. The ECU controls the injection time and frequency as well as the actuation energy that imposes the needle stroke. GDI requires injection time of the order of 0.5–5 ms (Hung et al., 2008). Throughout the study this time is kept constant and equal to 2 ms. The injection frequency is maintained at 0.2 Hz and the needle stroke energy at 63% of the full scale corresponding to a needle stroke of the order of 35 μm.

Fig. 2 shows an image of the liquid flow issuing from the GDI injector. This image was obtained for a medium injection pres-

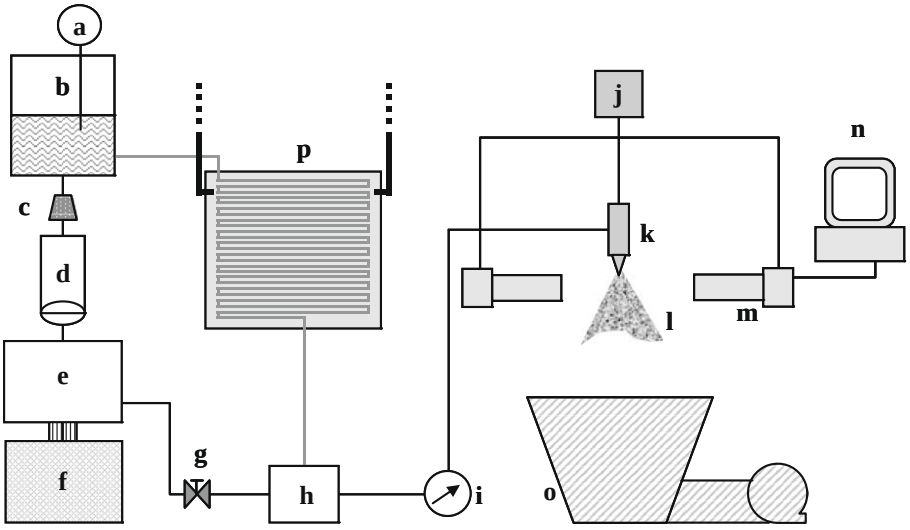

Fig. 1. Experimental setup. a – thermocouple, b – fuel tank, c – filter, d – LP pump, e – HP pump, f – electric motor, g – valve, h – pressure regulator, i – pressure sensor, j – Engine Control Unit (ECU), k – injector, l – spray, m – the Malvern Spraytec, n – PC, o – extraction system, p – heat exchanger.

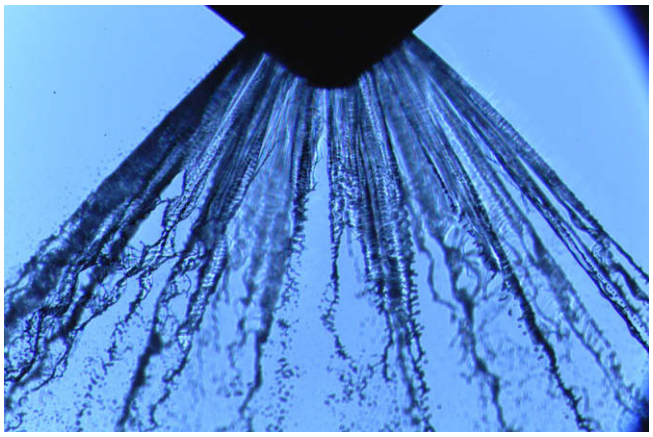

Fig. 2. Atomization mechanism of the liquid sheet (ΔP_i = 4 MPa).

sure (ΔP_i = 4 MPa). The liquid sheet angle at the nozzle is of the order of 80°. It is known that the angle of conical liquid sheet issuing from pressure swirl atomizer depends on the ambient pressure (Egermann et al., 1999). The present liquid sheet does not result from an intensive swirling internal flow and, consequently, its angle is not affected by ambient pressure changes. This characteristic feature constitutes an advantage as far as the application is concerned. As it can be seen in Fig. 2, the absence of a rotating component of velocity in the liquid sheet formation considerably modifies the atomization mechanism. The conical liquid sheet rearranges as a succession of longitudinal streaks that individually atomize from the development of very small interfacial perturbations similar to those observed on turbulent liquid sheets (Grout et al., 2007). We see in Fig. 2 that two consecutive streaks can be connected by a thin liquid lamella. The coexistence of two liquid structures in the atomization mechanism (streaks and lamellas) can favor the production of two distinct drop-size populations. This atomization mechanism is dominant when the injection pressure is greater than 4–5 MPa according to the needle stroke. The sprays resulting from this atomization mechanism show a hollow structure, namely, in planes perpendicular to the downstream direction, the droplets are distributed within an annular region whose diameter increases with the distance from the nozzle.

2.2. Diagnostic and protocol

The laser-diffraction equipment used to measure the drop-size distribution is the Spraytec 2007 from Malvern, which has been specifically conceived to investigate highly transient dense sprays. The wavelength and diameter of the laser beam are 632.8 nm and 10 mm, respectively. A series of 36 diodes equips the receiver. The collecting lens has a focal length equal to 300 mm and the measurable diameter range is 0.5–600 μm. The spatial arrangement of the Spraytec is schematized in Fig. 3. The distances d_l, d_D and L_s indicated in this figure are equal to 50, 180 and 84 mm, respectively. These distances are kept constant except otherwise mentioned.

The measurements are performed at the greatest available acquisition rate, i.e., 10 kHz. Fig. 4 shows the temporal evolution of transmission (expressed in percentage) for several injections and an injection pressure ΔP_i equal to 10 MPa. The initial time corresponds to the time when the electronic command is sent to the injector. After a delay of the order of 1 ms that corresponds to the time required for the spray to reach the laser beam, the transmission experiences a sharp decrease between 1 and 2 ms and then shows a less pronounced decrease between 2 to 4 ms. During this latter time interval, oscillations of the transmission are evidenced. At around 4 ms, the transmission reaches a minimum value (T_{min}) and then continuously increases at a rate that decreases with time. Contrary to other injection systems (see Boyaval and Dumouchel, 2001, for instance), the minimum transmission

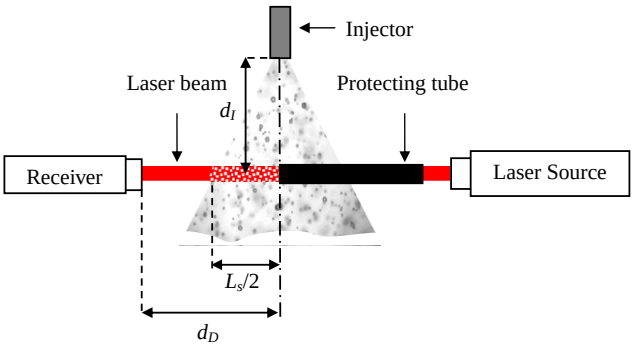

Fig. 3. Malvern Spraytec arrangement.

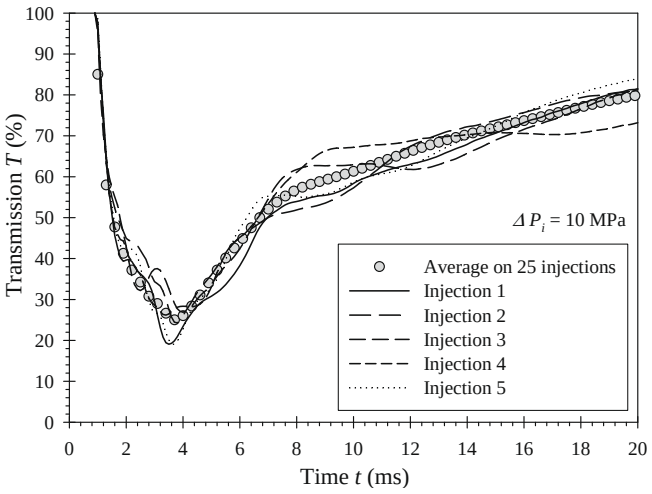

Fig. 4. Temporal evolution of the transmission during the injection. Influence of the injection event (ΔP_i = 10 MPa).

does not spread over a time interval. A low and constant transmission is commonly interpreted as the passage in the laser beam of the spray body, that is, the spray not affected by the injection transient phases. The absence of spray body in the present situation is the consequence of the use of very short injection time.

Fig. 4 shows that the temporal evolution of the transmission slightly differs from one injection to another. The exact reason for this has not been identified but the high sensibility of the spray to ambient air draft could be the main factor at the origin of this lack of reproducibility. To avoid this problem in the analysis, we decided to average the measurement on 25 injections. For an injection pressure of 10 MPa, the temporal evolution of the average transmission is shown in Fig. 4. For each time delay, averaging is also performed on the scattered light intensity distributions recorded during the 25 injections and the resulting drop-size distribution is calculated from this average intensity distribution. Minimum transmissions T_{min}, light intensity distributions and drop-size distributions presented and analyzed in this paper all result from this averaging process. It was checked that the drop-size distribution calculated this way was equal to that obtained by averaging the 25 drop-size distributions.

Vignetting and laser beam steering are two undesirable phenomena that affect laser-diffraction measurements. Before any analysis, preliminary tests are required to estimate their respective influence on the measurements. Vignetting designates the phenomenon by which scattered light escapes from the collection angle. It affects the detection of the drops that have the greatest diffracted light angle, i.e., the small particles. In consequence, the measured drop-size distribution underestimates the small-drop population. Three parameters control the vignetting effect: the size of the smallest drops to be measured, the distance between the spray and the collecting lens (working distance) and the lens focal length. The working distance should not be greater than 1.5 times the focal length lens. This limit must be shortened if very small drops have to be measured. As described in the previous section, the droplets are distributed within an annular region. Thus, along its optical path, the laser beam encounters two independent spray portions located at 222 mm and 138 mm from the collecting lens. Expecting a high proportion of small droplets in the present sprays, vignetting effects due to the spray portion located at 222 mm from the lens is suspected. To quantify this, the following preliminary test is performed.

This test consisted in measuring the left portion of the spray only as a function of the working distance. To achieve this, a tube is used to protect the incident light from the right-spray portion (see Fig. 3). Measurements were performed for d_D = 130, 180 and 260 mm corresponding to a working distance equal to 88, 138 and 218 mm, respectively. Fig. 5 compares the normalized light intensity distributions obtained for the three distances and for an injection pressure equal to 10 MPa. These intensity distributions are those recorded at the smallest transmission, denominated T'_{min} for the half-spray measurements (left portion) and which is equal to 43% for this injection pressure. Fig. 5 shows that the three intensity distributions are very much alike all over the diode series except for the three last external diodes (34–36), which are those that detect the light scattered by the small droplets. The light intensities collected by these diodes decrease as the distance d_D increases, which is a clear manifestation of vignetting effect.

Throughout the experimental work, the distance d_D was kept constant and equal to 180 mm since a shorter distance was inappropriate because of drop impaction on the Fourier lens at high injection pressure. With this distance, Fig. 5 shows that vignetting affects the left-spray portion measurement on diode 36 only and the right-spray portion measurement (corresponding to d_D = 260 mm in Fig. 5) on diodes 34–36. Thus, as diode 36 is always affected by vignetting effect, it is ignored in the following. Concerning diodes 34 and 35, half-spray normalized intensity reports a good proportion of the intensity they collect. These intensities are going to be used to correct the right-spray portion as explained in the next section. In consequence these two diodes are always kept in the following.

Beam steering effect is the manifestation of light scattered because of a refractive index gradient in the gas phase. The mathematical inversion procedure interprets this supplementary scattered light as being due to the presence of drops and calculates the drop-size distribution accordingly. Beam steering deviates light at small angles and mainly affects the proportion of light detected by the first inner diodes, i.e., those sensitive to the big drops. In consequence, the drop-size distribution overestimates the big-drop population and may exhibit a supplementary peak in this range of droplets. Such a peak was often detected in the present work. A characteristic feature of the presence of beam steering is a peak of light intensity detected by the first diode. The normalized intensity distributions shown in Fig. 5 have this characteristic feature. Beam steering effects must be therefore suspected.

A refractive index gradient in the surrounded gas flow can be caused by temperature gradients or by the presence of liquid vapor. The presence of temperature gradients is disregarded in the

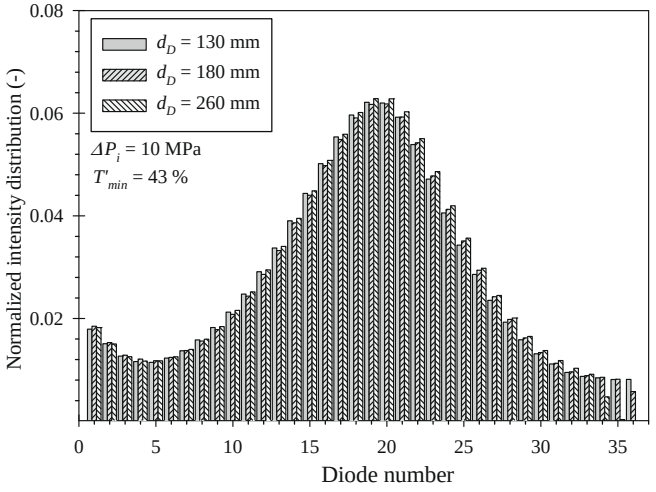

Fig. 5. Detection of vignetting effects (ΔP_i = 10 MPa).

present experiments. Liquid vapor can be generated either by cavitation of the internal flow or by small droplets vaporization. Considering the high injection pressures and the small nozzle outlet section, liquid cavitation cannot be excluded as well as vaporization because of the expected high proportion of small drops. Decreasing the injection pressure contributes to reduce these two phenomena and should therefore diminish the beam steering effects. Half-spray measurements were conducted for several injection pressures. The resulting normalized intensity distributions are compared in Fig. 6 where it appears that the peak of intensity detected by the first diode decreases with the injection pressure. Therefore, beam steering affects the measurements and explains the detection of a supplementary peak in the big-drop population. To avoid the bias caused by beam steering, Malvern recommends ignoring the intensity collected by the first diodes. The number of diodes to be ignored is a function of the operating conditions. In the present work, we found that ignoring the nine first diodes was required to ensure the disappearance of the big-drop supplementary peak for all operating conditions. This diode reduction was systematically applied.

In conclusion, spray drop-size characteristics are calculated on the basis of the intensity distribution collected by the diode range [10–35].

3. Results

3.1. Influence of light multiple scattering and vignetting effects

As reminded in Section 1, several investigations reported a non-negligible influence of multiple light scattering when the transmission is less then 40%. When both spray portions are measured (full-spray measurement) this limit is reached for an injection pressure equal to 6 MPa. This pressure becomes 11 MPa when one portion of the spray is measured (half-spray measurement). Therefore, in the range of pressure of interest [15 MPa; 20 MPa] light multiple scattering effects are expected. Comparing the characteristics of the measured spray with those of the actual spray can identify these effects. This can be achieved by comparing full and half-spray measurements provided that the half-spray measurement transmission is equal to or greater than 40%. This protocol, similar to the one used by Boyaval and Dumouchel (2001), makes sense if the protecting tube does not affect the spray characteristics and if these characteristics are axisymmetric. To control this, two preliminary tests are performed.

The first test consists in comparing the transmissions of full and half-spray measurements. The transmission can be expressed as:

$$T = e^{-\tau L_s} \tag{2}$$

where the spray turbidity τ depends on the spray spatial density and on the scattering properties of the particles, and L_s is the width of the measured spray. The spray axisymmetry should imply a spray length divided by 2 when measuring one spray portion instead of two. In consequence, according to Eq. (2), the transmission T' of the half-spray measurement is expected to be related to the full-spray measurement transmission T by:

$$T' = \sqrt{T} \tag{3}$$

Fig. 7 compares the minimum transmission T_{min} and T'_{min} for a wide range of injection pressures. Eq. (3) is plotted in this figure also. The agreement between the calculation and the measurements is acceptable. We note however that the measured transmissions T'_{min} are slightly smaller than the calculated ones. This is representative of an increase of the number of droplets in the measuring volume during the half-spray measurements. Impaction of drops on the tube and the creation of recirculation zones could explain this drop number increase. However, this undesirable effect remains limited.

The second test consists in comparing the full and half-spray drop-size distributions obtained at the minimum transmission for an injection pressure that guarantees no light multiple scattering effects for both measurements. Such comparisons are presented in Fig. 8 for two injection pressures (ΔP_i = 1 MPa and 5.47 MPa). The results show that half and full-spray drop-size distributions agree very well. It has to be mentioned that these measurements were conducted along several diameters of the spray by rotating the injector. In each situation, full and half-spray drop-size distributions agreed as well as those shown in Fig. 8. Note that the impact of vignetting effect identified above on full-spray measurement is undetectable at these low injection pressures. These preliminary tests demonstrate that the protecting tube introduces a negligible perturbation and that the spray drop-size distribution is axisymmetric enough to consider the half-spray distribution representative of the whole spray distribution.

As indicated in Section 1, previous investigations identified the presence of light multiple scattering by considering the evolution of characteristic drop diameters or of the light intensity distribution with the transmission. Both are considered here. First, we look

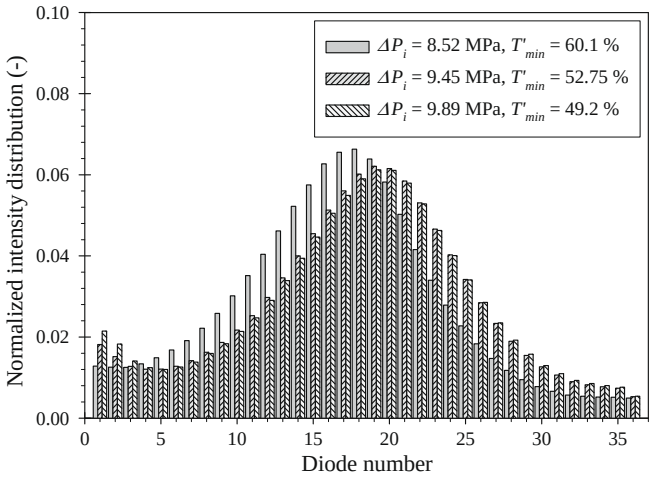

Fig. 6. Detection of beam steering effects (ΔP_i = 10 MPa).

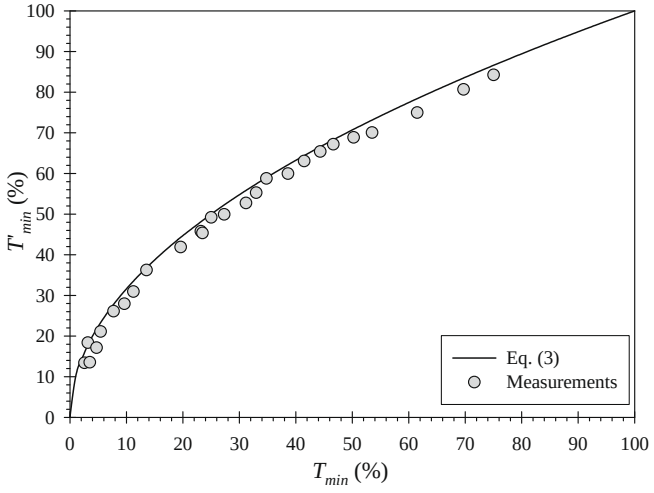

Fig. 7. Correlation between the full-spray measurement minimum transmission T_{min} and the half-spray measurement minimum transmission T'_{min}. Comparison with Eq. (3).

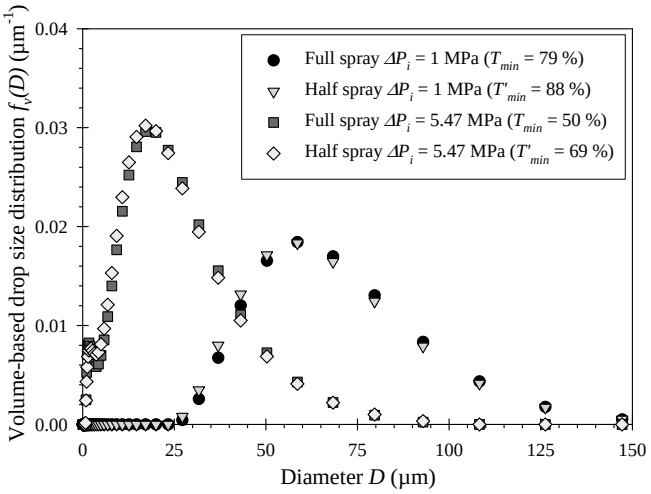

Fig. 8. Comparison between full and half-spray drop-size distributions (ΔP_i = 1 MPa and ΔP_i = 5.47 MPa).

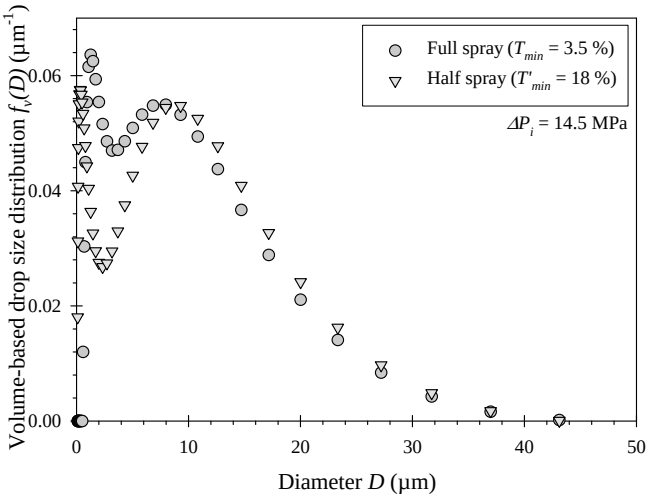

Fig. 10. Comparison between full-spray and half-spray drop-size distributions at ΔP_i = 14.5 MPa.

at the full-spray diameter/half-spray diameter ratios for diameter $D_{v0.5}$, $D_{v0.9}$, D_{43} and D_{32} as a function of the full-spray transmission T (Fig. 9). For T > 40%, the diameter ratios are of the order of 1 as expected. Then, when T is comprised between 40% and 14%, the ratios deviate from 1 and increase. When the transmission further decreases, the $D_{v0.5}$, $D_{v0.9}$ and D_{43} ratios mainly decrease whereas the D_{32} ratio first decreases and then sharply increases to reach the value 1.3 at the smallest transmission. These unexpected evolutions of diameter ratio are due to a combination of vignetting and multiple light scattering effects. To illustrate this, Fig. 10 compares the full and half-spray drop-size distributions obtained at ΔP_i = 14.5 MPa and corresponding to the smallest transmission T_{min}. This figure shows that the tail of the full-spray distribution is below the one of the half-spray distribution, which evidences the impact of light multiple scattering between the two measurements. Note that the half-spray transmission T'_{min} is below 40% and that the corresponding distribution may be also affected by light multiple scattering. However, these effects are less than for the full-spray measurement whose transmission is far less. On the other side of the distribution, we note that the small-drop population reported by the full-spray measurement is less than the one of the half-spray measurement. This difference is due to vignetting effects. Thus, the specific variations of the diameter ratios shown in Fig. 9 are the manifestation of the combination of vignetting and light multiple scattering effects that have an opposite influence on the characteristics drop diameters. The diameter ratios greater than 1 when 14% < T_{min} < 40% reveal that vignetting is more effective than light multiple scattering in this range of working conditions.

Second, we look at the series of coefficients $\kappa_i(T)$ defined by:

$$\kappa_i(T_{\min}) = \frac{I_i(T_{\min})}{I_i(T'_{\min})}, \quad i = 10, 11, \ldots, 35 \tag{4}$$

where i denotes the diode number. In Eq. (4), $I_i(T_{min})$ is the normalized light intensity distribution of the full-spray measurement and $I_i(T'_{min})$ is the corresponding distribution of the half-spray measurement. Fig. 11 shows the evolution of the coefficients $\kappa_i(T_{min})$ with the transmission T_{min} for a few diodes. For T_{min} > 20%, the coefficients $\kappa_i(T_{min})$ are rather independent of the transmission. They are equal to 1 for diodes 10–34 and less than 1 for diode 35. This latter result is the manifestation of vignetting effects. Note that when measuring both spray portions (full-spray measurement) the influence of these effects on the intensity collected by diode

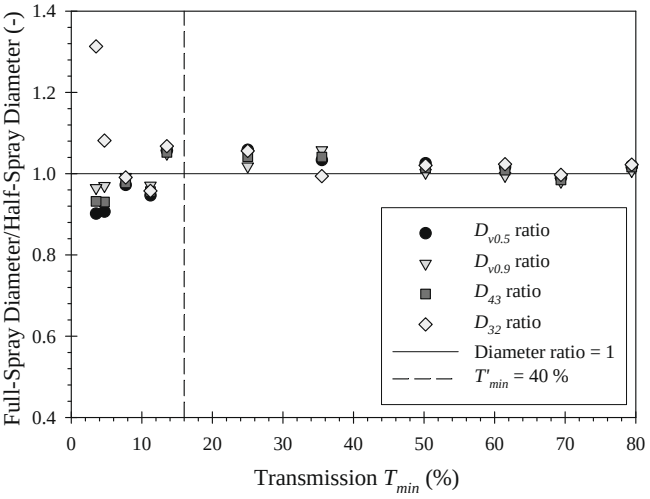

Fig. 9. Evolution of full-spray diameter/half-spray diameter ratio as a function of the transmission T_{min}.

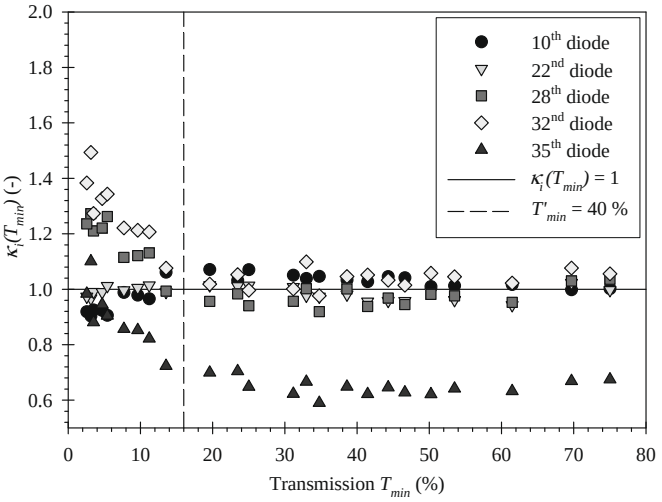

Fig. 11. Evolution of the coefficients κ_i as a function of the full-spray measurement minimum transmission. Influence of the diode.

34 is negligible. For low transmissions (less than 20%), the coefficients κ_i deviate from the constant value and become dependent on the transmission. The variation rate of the coefficient with the transmission is a function of the diode. For internal diodes (up to the 22nd diode), κ_i decreases as T_{min} decreases whereas for the external diodes (from the 28th to the 35th diodes), κ_i increases as T_{min} decreases. Such variations of the coefficients κ_i are those expected from light multiple scattering effects. However, as discussed above, vignetting effects compensate light multiple scattering effects and the measurements must be corrected from both effects. The correction procedure presented in the next section is developed for this purpose.

3.2. Multiple light scattering and vignetting correction procedure

A corrected intensity distribution $\tilde{I}_i(T)$ is calculated from the *full-spray intensity distribution* $I_i(T)$ by the relation:

$$\tilde{I}_i(T) = \frac{I_i(T)}{\tilde{\kappa}_i(T)} \tag{5}$$

introducing the correction factor series $\tilde{\kappa}_i(T)$. If the half-spray measurement is not affected by multiple scattering, the corrected intensity $\tilde{I}_i(T)$ must be equal to the intensity $I_i(T')$. Thus, in this condition, the correcting factors are equal to the coefficients introduced by Eq. (4), i.e., $\tilde{\kappa}_i(T) = \kappa_i(T)$. Note that this correction factor series also corrects from vignetting effects. Now, if the half-spray measurement is affected by multiple scattering effects, the intensity distribution $I_i(T')$ requires to be corrected. However, the correction factors series for the half-spray measurements is unknown.

As reminded in Section 1, light multiple scattering effects depend on the transmission as well as on the spray characteristics. Considering Rosin–Rammler drop-size distribution, Felton et al. (1985) demonstrated that light multiple scattering effects were mainly dependent on the transmission and on the dispersion parameter of the distribution and were almost independent of the size parameter of the distribution. As demonstrated by Lefebvre (1989), Rosin–Rammler distributions show a unique relationship between the dispersion parameter and the relative span factor Δ_v. Thus, Felton et al.'s (1985) conclusion can be reformulated as follows: the multiple light scattering effects are mainly dependent on the transmission and on the span factor. On the other hand, Gülder (1990) determined correction factors for the Sauter mean diameter D_{32} as a function of the transmission and of D_{32} and found that the transmission dominated the change in correction factor. In agreement with Felton et al.'s (1985) conclusion, this finding illustrates the negligible influence of the size parameter on the light multiple scattering effects. Fig. 12 shows the evolution of the span factor of the full and half-spray measurement as a function of their transmission T_{min} and T'_{min}, respectively. We note in this figure that the functions $\Delta_v(T)$ are very much alike. Therefore, using Felton et al.'s (1985) conclusions, we assume that the light multiple scattering effects are mainly dependent on the transmission in our work and that the same correction factor series can be used for the full and half-spray intensity distributions. At low transmission values, Fig. 12 shows that the span factor of the half-spray distribution is slightly greater than the one of the full-spray distribution. According to Felton et al. (1985) this difference indicates that the above assumption under corrects the half-spray distribution. Using Felton et al.'s results, we estimated that the error made for the corrected span factor is never greater than 10%. This error is sufficiently low to accept the proposed assumption.

Since vignetting never affects half-spray measurements, the corrected intensity distribution $\tilde{I}_i(T)$ can be rewritten as:

$$\tilde{I}_i(T) = \frac{a_i I_i(T')}{\tilde{\kappa}_i(T')} \tag{6}$$

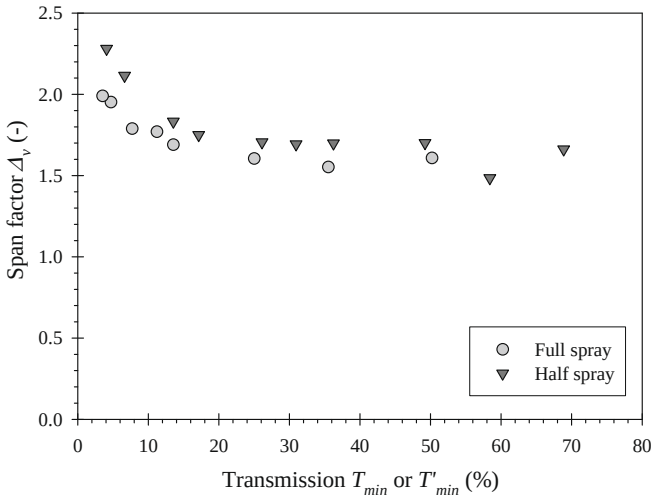

Fig. 12. Evolution of the full and half-spray span factor Δ_v as a function of the respective transmission.

where the coefficients a_i are defined by:

$$a_i = \lim_{T \to 100} (\kappa_i(T)) \tag{7}$$

These coefficients are equal to 1 for all diodes except for diode 35 for which $a_i = 0.64$. The series of correction factors $\tilde{\kappa}_i(T)$ can be derived from Eqs. (3)–(6). It comes:

$$\tilde{\kappa}_i(T) = \kappa_i(T) \frac{\tilde{\kappa}_i(\sqrt{T})}{a_i} \tag{8}$$

This equation is implicit. By applying it for successive values of the transmission it can be rewritten as:

$$\tilde{\kappa}_i(T) = a_i \prod_{j=0}^{n} \frac{\kappa_i((T)^{1/2^j})}{a_i} \tag{9}$$

When multiple scattering effects do not affect the half-spray measurement, the first term of the series is required only, i.e., $n = 0$ because the successive terms of the series for $n > 0$ are equal to 1. When the half-spray measurement has to be corrected once, the two first terms of the series are required, i.e., $n = 0$ and 1, the series terms for higher n being all equal to 1. Therefore, the application of Eq. (9) requires a parameter n high enough so that the last term of the series in the right-hand side of the equation is equal to 1. This condition is always satisfied when $T^{1/2^n}$ is greater than 0.95. Thus, the value of n depends on the transmission and is determined on the basis of the following condition:

$$T^{1/2^n} > 0.95 \tag{10}$$

The correction factor series given by Eq. (9) corrects from light multiple scattering and vignetting effects and therefore must be used for full-spray measurements only. Full-spray measurements were performed for injection pressures up to 14.5 MPa only. For greater injection pressures, the transmissions were less than 3.5% and the light intensity distributions were unexploitable. However, for greater injection pressures (between 15 MPa and 20 MPa) half-spray measurements are still possible. Since vignetting does not affect half-spray measurements, the appropriate correction factor series to be applied to these measurements must be reformulated. According to Eq. (9), it comes:

$$\tilde{\kappa}'_i(T') = \prod_{j=1}^{n} \frac{\kappa_i\left((T')^{1/2^{(j-1)}}\right)}{a_i} \tag{11}$$

In order to simplify the calculation of the correction factor given by Eqs. (9) and (11) for any value of the transmission, the coefficients κ_i (Eq. (4) and Fig. 11) are modeled using the following expression:

$$\kappa_i(T) = a_i - (a_i - \kappa_i(0))e^{\gamma_i T} \tag{12}$$

where a_i are defined by Eq. (7) and are obtained from Fig. 11. For each diode i, two parameters have to be determined, namely, $\kappa_i(0)$ and γ_i. This is achieved by rewriting Eq. (12) as:

$$ln(|a_i - \kappa_i(T)|) = ln(|a_i - \kappa_i(0)|) + \gamma_i T \tag{13}$$

and by plotting ln $(|a_i - \kappa_i(T)|)$ as a function of T. This plot is shown in Fig. 13 for three different diodes. For each of them, we note that the linear dependence expressed by Eq. (13) is satisfactorily observed. For each diode, the slope of the linear regression gives the parameter γ_i and the ordinate for $T = 0$ returns the parameter $\kappa_i(0)$.

Thus, the corrections factor series (Eq. (9) or (11)) is calculated using the analytical expression of the coefficients $\kappa_i(T)$ (Eq. (12)) and paying attention that the parameter n satisfies the condition expressed by Eq. (10). As an illustration, the resulting coefficient series $\tilde{\kappa}_i(T)$ (Eq. (9)) is shown in Fig. 14 for selected diodes.

The correction process developed here is actually a generalization of the procedure proposed by Boyaval and Dumouchel (2001) that consisted in a double correction only, i.e., $n = 1$ in Eq. (9) or (11). A comparison between the second and nth order correction procedures was conducted. We found that the two procedures reported the same result when the transmission T was greater than 10%. This corresponds to an injection pressure equal to 11 MPa. Thus, the second order correction procedure was sufficient in Boyaval and Dumouchel's work where the injection pressure did not exceed 8 MPa. However, for injection pressures greater than 11 MPa, the results obtained from the second and nth order correction procedures were different. The nth order approach accentuated the level of correction. This is illustrated in Fig. 15 for the injection pressure equal to 20 MPa. This figure shows the benefit in using an nth order correction for high injection pressures.

The nth order correction procedure is now applied to evaluate the limit transmission under which light multiple scattering affects the measurements. To achieve this, we correct the full-spray measurements from vignetting effects only by dividing the intensity collected by each diode i by the coefficient a_i introduced by Eq. (7). Thus, the resulting full-spray characteristics are affected by light multiple scattering only. Then, we compare these spray characteristics with those of the actual spray obtained from the application of the nth order correction procedure. Fig. 16 shows the vignetting-free full-spray diameter/actual-spray diameter ratios as a function of the transmission for four different diameters, namely, $D_{v0.5}$, $D_{v0.9}$, D_{43} and D_{32}. Since the full-spray measurements were corrected from vignetting effects, the evolution of the diameter ratios as a function of the transmission is the manifestation of light multiple scattering effects only. This is consistent with the results presented in Fig. 16 that show that the diameter ratios are first constant and equal to 1 and then decrease when the transmission decreases. Note that the transmission from which the diameter ratios deviate is a function of the considered diameter: the D_{32} and $D_{v0.5}$ ratios start to decrease for a transmission less than 40% whereas the decrease of the $D_{v0.9}$ ratio is effective when the transmission is less than 10%. These behaviors agree with Paloposki and Kankkunnen's findings (1991). Based on the results shown in Fig. 16, we can conclude that light multiple scattering starts affecting laser-diffraction measurement when the transmission is less than 40%. As reminded in Section 1, this limit is identical to the one reported by several previous investigations. This agreement gives credit to the empirical correction procedure developed here.

We now examine the influence of light multiple scattering on spray drop-size distribution. The series of Fig. 17 compares the vignetting-free full-spray drop-size distribution with the actual-

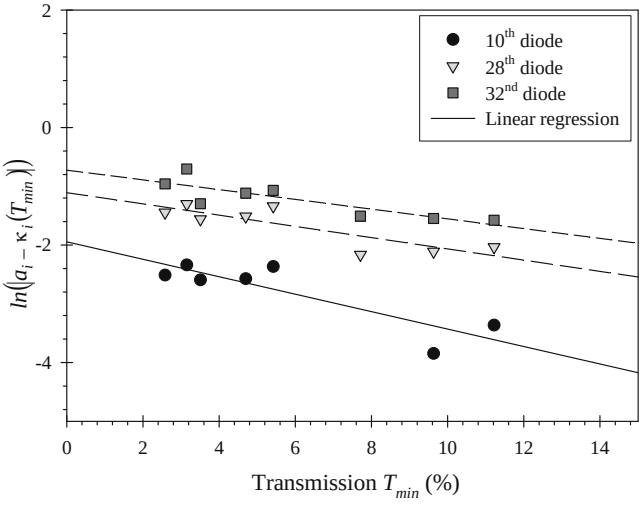

Fig. 13. Model for the coefficients κ_i. Plot of Eq. (13) for three diodes.

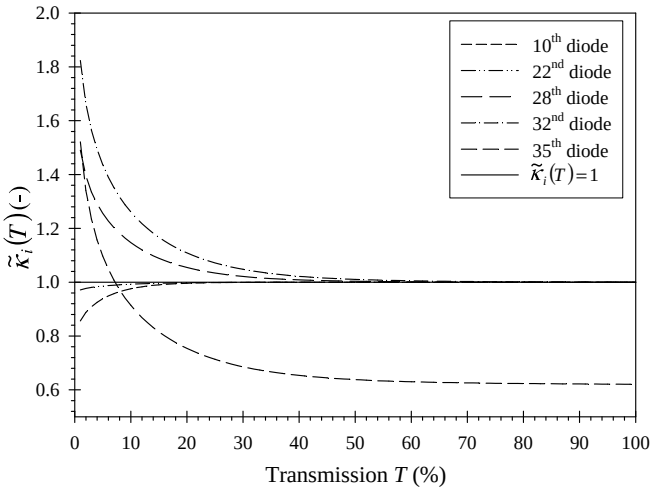

Fig. 14. Evolution of the correction factors $\tilde{\kappa}_i(T)$ (Eq. (9)) as a function of the full-spray transmission T.

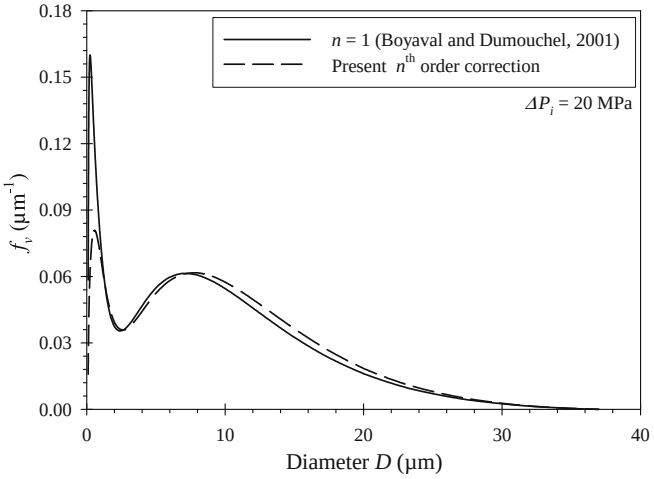

Fig. 15. Comparison Boyaval and Dumouchel (2001) second order correction ($n = 1$) and the present nth order correction ($\Delta P_i = 20$ MPa).

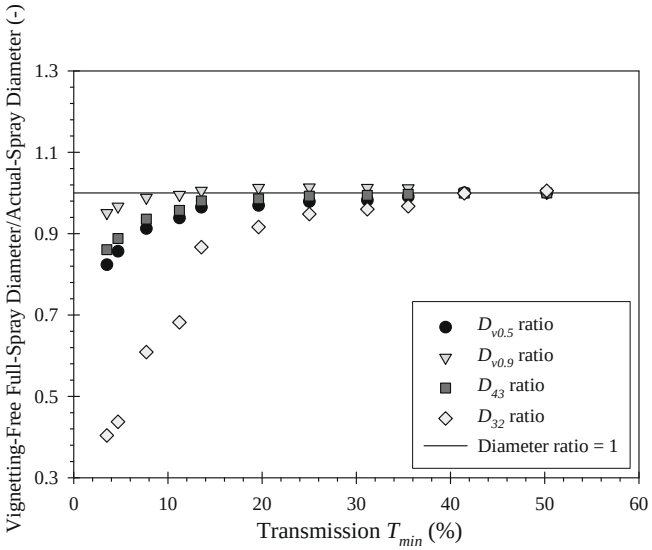

Fig. 16. Evolution of vignetting-free full-spray diameter/actual-spray diameter ratio as a function of the transmission T_{min}.

spray drop-size distribution resulting from the application of the *n*th order correction procedure. These figures show that the vignetting-free distribution is always left shifted compared to the actual distribution. This behavior corresponds to the expected influence of multiple light scattering. For $T = 31\%$ ($\Delta P_i = 9.45$ MPa, Fig. 17a) the shift is moderate but is clearly observable for drop diameter less than 20 μm. When the transmission decreases, this shift becomes more and more pronounced (see Fig. 17b and c, $\Delta P_i = 10.75$ MPa, $T = 20\%$, and $\Delta P_i = 14.5$ MPa, $T = 3.5\%$, respectively). Fig. 17 also show the drop-size distribution obtained from the application of the optional Malvern light multiple scattering correction algorithm. Since this algorithm is not supposed to correct vignetting effects, it was applied on vignetting-free full-spray measurements. It can be seen that the distribution reported by the Malvern correction algorithm always overcorrects the measurements. For transmission down to 31%, the disagreement appears moderate (Fig. 17a) but it becomes very important for transmission less than 20% (Fig. 17b and c). Note that for the three applications shown here, the correction algorithm eradicates all droplets with a diameter less than 2–3 μm. When the injection pressure is equal to 14.5 MPa (Fig. 17c) the absence of such drops is unrealistic. As reminded in Section 1, the model on which this correction algorithm is based assumes isolated particle light scattering and spray characteristics (concentration and drop-size distribution) uniformly distributed in space. The characteristics of the present sprays are not uniformly distributed in space. Furthermore, at high injection pressure, one may wonder whether a reduction of interparticle spacing would cause the scattering characteristics of a particle to depend on the position and sizes of adjacent particles. In conclusion, it is not recommended to use the Malvern correction algorithm for the present sprays.

3.3. Example of applications

In this section, applications of the *n*th order correction procedure are performed to determine and investigate the drop-size distribution of the spray produce by the high-pressure GDI injector. Fig. 18 shows a series of volume-based drop-size distributions for an injection pressure ranging from 10 MPa to 20 MPa. These distributions are those obtained at the minimum transmission. We note a clear evolution of the drop-size distribution with the injection pressure. At 10 MPa, the distribution is mainly mono-modal, i.e., it shows a single peak. When the injection pressure increases, the drop-size distribution shifts towards the small-drop population and a second peak develops in the 2 μm diameter region.

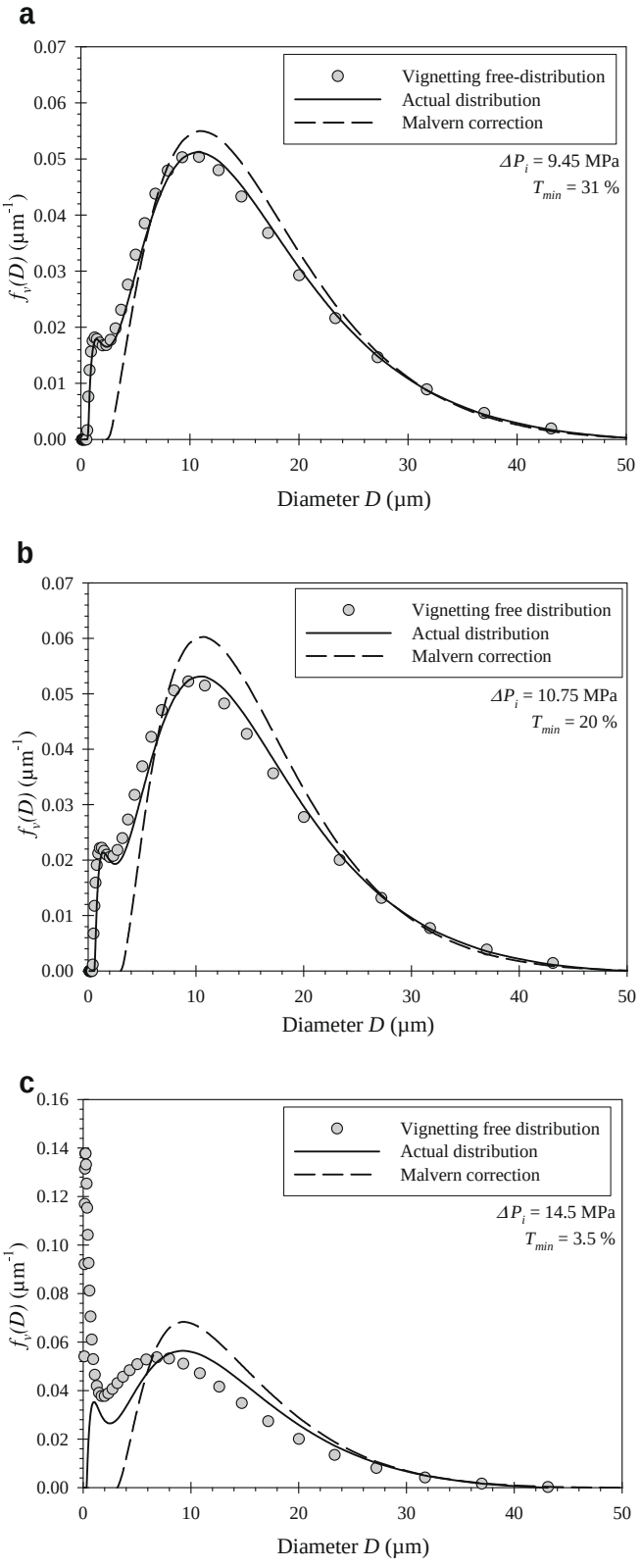

Fig. 17. Comparison between the vignetting-free full-spray drop-size distribution, the actual-spray drop-size distribution and the drop-size distribution obtained from the application of the Malvern correction algorithm. a – $\Delta P_i = 9.45$ MPa, b – $\Delta P_i = 10.75$ MPa, c – $\Delta P_i = 14.5$ MPa.

The height of this peak increases with the injection pressure. As mentioned above, the atomization mechanism of the conical sheet issuing from the injector involves several liquid structures such as longitudinal ligaments and thin liquid lamellas. These liquid structures and their respective atomization mechanism have different characteristic length scales and are likely to produce distinct drop populations. The bi-modal drop-size distributions obtained here are therefore not unrealistic. One of the important specifications a GDI spray must fulfill is the absence of 45 μm drops (Zhao et al., 1997). With the present GDI injector used with a 63% needle stroke energy, this condition is reached for injection pressures greater than 15 MPa.

The high acquisition rate of the Malvern Spraytec 2007 constitutes an advantage for the characterization of highly transient sprays as those studied here. The diagnostic is able to perform measurements with a temporal resolution of 0.1 ms and to follow the drop-size distribution temporal evolution during one injection. An example of this is shown in Fig. 19 for the greatest injection pressure (ΔP_i = 20 MPa). In order to facilitate the reading of this 3D plot, only one distribution by four is represented (the time step between two consecutive distributions is equal to 0.4 ms) and a log-scale has been used for the diameter axis. The temporal evolution of the transmission is plotted also. This figure shows that the drop-size distribution is bi-modal all over the time. Between 2 ms and 4 ms after the injection command, the small-drop population mode is the most developed. Note that this time interval corresponds to the smallest transmissions, which denotes the passage in the measurement volume of a high-density spray. Thus, the drop-size distributions measured during this time interval characterize the greatest proportion of injected liquid volume. After 5 ms, the drop-size distribution moderately varies whereas the transmission continuously increases. This characterizes the cloud of drops in suspension after the passage of the main spray.

The result shown in Fig. 19 was obtained from measurements averaged on 25 injections. The averaging process was a necessary step to develop a statistically representative correction procedure. However, this correction procedure can be applied on individual injection measurements to give the cycle-to-cycle variations of the drop-size distribution. This result, not shown in the present work, constitutes an important characteristic of GDI injector performances. Up so far, the Malvern Spraytec is probably the sole instrument able to report this valuable information.

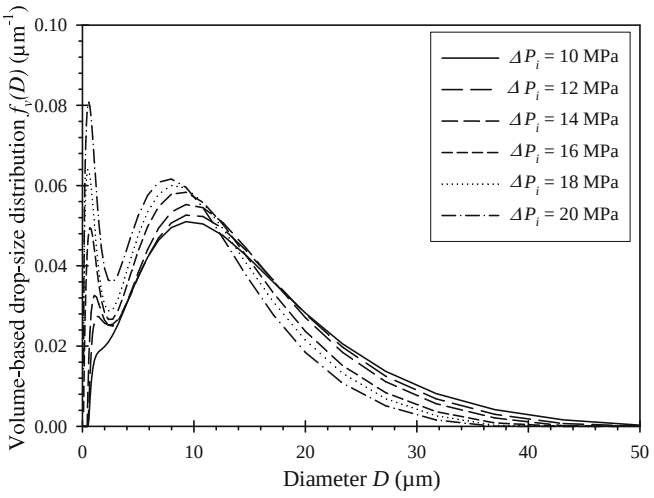

Fig. 18. Evolution of the drop-size distribution as a function of the injection pressure.

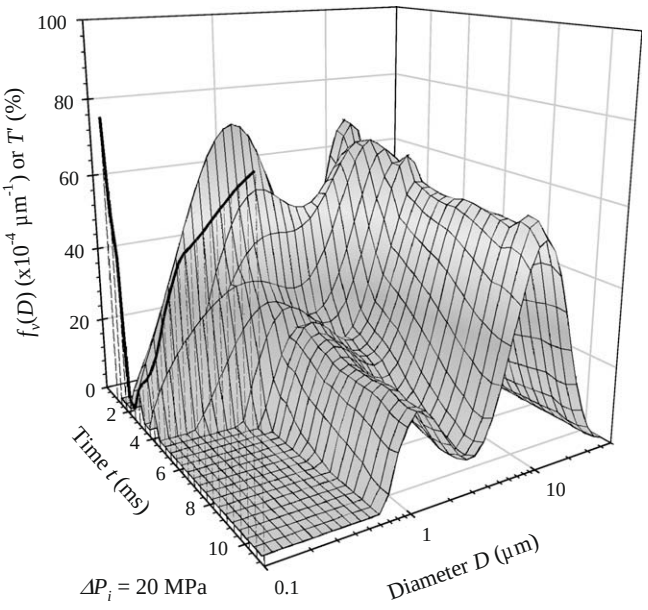

Fig. 19. Temporal evolution of the drop-size distribution and of the transmission during one injection (ΔP_i = 20 MPa).

4. Conclusion

The present investigation details a practical use of a laser-diffraction technique to characterize complex-spray drop-size distribution; the Malvern Spraytec 2007. This instrument is rather easy to operate and is able to perform high acquisition rate measurements. It is therefore recommended to study highly transient sprays such as those investigated here and produced by GDI injectors. Besides being highly transient, these sprays are dense, mainly composed of very small drops, large and heterogeneously distributed in space, each of these characteristics being a potential source of measurement bias. The phenomena that can affect the measurement are the beam steering, the vignetting and the light multiple scattering effects. The present experimental protocol includes the identification of the presence of these phenomena and an empirical correction procedure to correct the measurements from light multiple scattering and vignetting effects.

This correction procedure is a generalization of Boyaval and Dumouchel's (2000, 2001) procedure developed for similarly structured sprays and is based on the comparison between half and full-spray measurement characteristics. Contrary to Boyaval and Dumouchel (2000, 2001) who determined correction factors for two spray characteristics, namely, the mean diameter D_{43} and the span factor Δ_v, correction factor series are determined to correct the light intensity collected by each diode. This allows whole drop-size distribution to be determined instead of a limited number of spray characteristics. The generalization concerns the order of the correction: the second order correction procedure due to Boyaval and Dumouchel (2000, 2001) has been extended here to the nth order. It is demonstrated that this extension increases the level of correction when the transmission is less than T = 10% corresponding to injection pressures greater than 11 MPa. The application of the nth order correction procedure reported that light multiple scattering effects are effective when the transmission is lower than 40%. This limit agrees with previous experimental results and thus gives credit to the correction model. Furthermore, it was demonstrated that the Malvern light multiple scattering algorithm is not adapted for the present sprays especially when the transmission is less than 30%.

The combination of the Spraytec performances and of the present correction procedure allows spray drop-size distribution to be

measured for injection pressure as high as 20 MPa and temporal evolution of the drop-size distribution during an injection to be investigated. Furthermore, it is important to emphasize that the determination of cycle-to-cycle temporal variations of the spray drop-size distribution is possible. As far as we know, the Malvern Spraytec is the sole instrument capable of giving this information. Of course, the application of the correction factor series obtained in this work is limited to the operating conditions that are those of the present study. However, this experimental protocol can be reproduced with ease on sprays produced from the disintegration of conical liquid flow as often encountered in GDI application.

References

Boyaval, S., Dumouchel, C., 2000. Experimental investigation on the measurement of drop size distribution of sprays produced by high-pressure swirl atomizers. In: Eighth International Conference on Liquid Atomization and Sprays Systems, Pasadena, CA, USA, July 2000.

Boyaval, S., Dumouchel, C., 2001. Investigation on the drop size distribution of sprays produced by high-pressure swirl injector. Measurements and application to the maximum entropy formalism. Part. Part. Syst. Char. 18, 33–49.

Cao, J., Brown, D.J., Rennie, A.G., 1991. Laser-diffraction particle sizing in dense suspensions and sprays with correction for multiple scattering. J. Inst. Energy 64, 26–30.

Corcoran, T.E., Hitron, R., Humphrey, W., Chigier, N., 2000. Optical measurement of nebulizer sprays: a quantitative comparison of diffraction, phase Doppler interferometry, and time of flight techniques. J. Aerosol Sci. 31, 35–50.

Dodge, L.G., 1984. Change of calibration of diffraction-based particle sizers in dense sprays. Opt. Eng. 23, 626–630.

Egermann, J., Ipp, W., Rabenstein, F., Wensing, M., Leipertz, A., 1999. Spray formation and evaporation of high pressure swirl atomizers for gasoline direct injection. In: Proceedings of ILASS-Europe'99, 5–7 July, 1999, Toulouse, France.

Felton, P.G., Hamidi, A.A., Aigal, A.K., 1985. Measurement of drop size distribution in dense sprays by laser diffraction. In: Proceedings of the ICLASS-85, London, England, Paper IVA/4/1.

Gomi, H., 1986. Multiple scattering correction in the measurement of particle size and number density by the diffraction method. Appl. Opt. 25, 3552–3558.

Grout, S., Dumouchel, C., Cousin, J., Nuglisch, H., 2007. Fractal analysis of atomizing liquid flow. Int. J. Multiphase Flow 33, 1023–1044.

Gülder, O.L., 1987. Multiple scattering effects in laser diffraction measurements of dense sprays with bi-modal size distributions. In: First Conference on Liquid Atomization and Spray Systems, ILASS Americas 87, Madison, USA.

Gülder, O.L., 1990. Multiple scattering effects in dense spray sizing by laser diffraction. Aerosol Sci. Technol. 12, 570–577.

Hamidi, A.A., Swithenbank, J., 1986. Treatment of multiple scattering of light in laser diffraction measurement techniques in dense sprays and particle fields. J. Inst. Energy 65, 101–105.

Harvill, T.L., Hoog, J.H., Holve, D.J., 1995. In-process particle size distribution measurements and control. Part. Part. Syst. Char. 12, 309–313.

Harvill, T.L., Holve, D.J., 1998. Size distribution measurements under conditions of multiple scattering with application to sprays. In: Proceeding of ILASS-Americas'98.

Hirleman, E.D., 1988. Modeling of multiple scattering effects in Fraunhofer diffraction particle size analysis. Part. Part. Syst. Char. 5, 57–65.

Hirleman, E.D., 1990. A general solution to the inverse near-forward scattering particle sizing problem in multiple scattering environment: Theory. In: Second International Congress on Optical Particle Sizing, Tempe, Arizona, USA, pp. 159–168.

Hung, D.L.S., Harrington, D.L., Gandhi, A.H., Markle, L.E., Parrish, S.E., Shakal, J.S., Sayar, H., Cummings, S.D., Kramer, J.L., 2008. Gasoline fuel injector spray measurement and characterization – a new SAE J2715 recommended practice. SAE Technical Paper Series, 2008-01-1068.

Lefebvre, A.H., 1989. Atomization and Sprays. Hemisphere Publishing Corporation, New York.

Paloposki, T., Kankkunen, A., 1991. Multiple scattering and size distribution effects on the performance of a laser diffraction particle sizer. In: Proceedings of the International Conference on Liquid Atomization and Spray Systems, ICLASS'91, Gaithersburg, USA, Paper 46, pp. 441–448.

Swithenbank, J., Beer, J.M., Taylor, D.S., Abbot, D., McCreath, C.G., 1977. A laser diagnostic technique for the measurement of droplet and particle size distribution. Experimental diagnostics in gas phase combustion systems. Prog. Astron. Aeron. 53, 421–447.

Triballier, K., Dumouchel, C., Cousin, J., 2003. A technical study on the Spraytec performances: influence of multiple light scattering and multi-modal drop-size distribution measurements. Exp. Fluids 35, 347–356.

Zhao, F., Harrington, D.L., Lai, M.C., 2002. Automotive gasoline direct-injection engines. SAE-R-315, pp. 51–116.

Zhao, F., Lai, M.C., Harrington, D.L., 1997. A review on mixture preparation and combustion control strategies for spark-ignited direct-injection gasoline engines. SAE Technical Paper No. 970627.